



**HAL**  
open science

## Improvement of 60 GHz transparent patch antenna array performance through specific double-sided micrometric mesh metal technology

Alexis Martin, Olivier Lafond, Mohamed Himdi, Xavier Castel

### ► To cite this version:

Alexis Martin, Olivier Lafond, Mohamed Himdi, Xavier Castel. Improvement of 60 GHz transparent patch antenna array performance through specific double-sided micrometric mesh metal technology. IEEE Access, 2019, 7 (1), pp.2256-2262. 10.1109/ACCESS.2018.2886478 . hal-01956234

**HAL Id: hal-01956234**

**<https://hal.science/hal-01956234>**

Submitted on 15 Dec 2018

**HAL** is a multi-disciplinary open access archive for the deposit and dissemination of scientific research documents, whether they are published or not. The documents may come from teaching and research institutions in France or abroad, or from public or private research centers.

L'archive ouverte pluridisciplinaire **HAL**, est destinée au dépôt et à la diffusion de documents scientifiques de niveau recherche, publiés ou non, émanant des établissements d'enseignement et de recherche français ou étrangers, des laboratoires publics ou privés.

Date of publication xxxx 00, 0000, date of current version xxxx 00, 0000.

Digital Object Identifier 10.1109/ACCESS.2017.DOI

# Improvement of 60 GHz transparent patch antenna array performance through specific double-sided micrometric mesh metal technology

**A. MARTIN, O. LAFOND, M. HIMDI AND X. CASTEL**

Univ Rennes, CNRS, IETR-UMR 6164, F-35000 Rennes, France

Corresponding author: O. Lafond (e-mail: olivier.lafond@univ-rennes1.fr).

This work is supported by the European Union through the European Regional Development Fund (ERDF), the Ministry of Higher Education and Research, the Région Bretagne, the Département des Côtes d'Armor and Saint-Brieuc Armor Agglomération, through the CPER Projects 2015-2020 MATECOM and SOPHIE / STIC & Ondes.

**ABSTRACT** This paper presents the performance of optically transparent  $4 \times 2$  microstrip patch antenna arrays operating at 60 GHz and made from double-sided micrometric mesh metal layers. A high level of optical transparency (higher than 80%) over the entire visible light spectrum coupled with a sheet resistance lower than  $0.5 \text{ ohm/sq}$  of the mesh metal films are achieved. Microwave performance of the transparent antenna arrays has been performed from two different mesh ground plane patterns and compared with those of an opaque antenna array made of double-sided continuous metal films. A gain value equal to 13.6 dBi at 58.0 GHz has been recorded, against 15.6 dBi at 59.7 GHz for the opaque antenna array. The influence of the mesh structure and mesh parameters of the ground plane is investigated and discussed.

**INDEX TERMS** Micrometric metal mesh, Microstrip antenna arrays, Millimeter wave antenna, Optically transparent antenna

## I. INTRODUCTION

The design and fabrication of optically transparent antennas printed onto glass substrates are of great interest to produce new communicating surfaces implemented on building windows, car glazing, or solar panels for example. With the advent of Internet of Things (IoT) and 5G, the needs for antennas with soft visual impact will grow in the next future. A first solution deals with the design of electrically small antennas [1], [2]. However these antennas provide weak radiation efficiency due to their small size. Another solution deals with the increase of the operating frequency to take advantage in antenna size reduction [3] at the expense to their technical complexity and development cost. In this frame, optically transparent antennas printed on transparent substrates present an alternative route to circumvent such problems. These antennas need nevertheless to be fabricated from transparent and conducting layers. The most usual materials belonging to the transparent and conducting oxide (TCO) family are indium tin oxide (ITO) [4] and zinc oxide [5]. However the provided sheet resistance  $R_s$  remains high for microwave

applications ( $R_s$  higher than  $8 \text{ } \Omega/\text{sq}$  [6]). Hybrid solutions based on TCO/metal multilayers are also available, such as ITO/Cu/ITO or ITO/Ag/ITO/Ag/ITO heterostructures [6]–[8], or the commercial AgHT films (ITO/silver multilayers printed on polyester substrates) [9]. Nonetheless, the sheet resistance, while improved, remains higher than  $1 \text{ } \Omega/\text{sq}$ . In addition, the optical transmittance of such materials varies in the visible light spectrum, causing a slight coloration of the conducting layer.

An alternative solution was specifically developed within IETR Institute since many years. It is based on printed micrometric mesh metal films [10]. Metal layer exhibits low sheet resistance value and apertures into the metal layer give the needed and constant optical transparency over the entire visible light spectrum. Metal thickness adjustment prevents any skin depth loss at the operating frequency, while keeping a high level of optical transparency. Micrometric mesh dimensions processing of the metal film provides soft visual impact of such samples, compared with that of grid layers, also called see-through devices or see-through antennas [11].

Indeed the micrometric mesh pattern is selected here to be non-visible at the *punctum proximum* of the ordinary human vision ( $d = 25$  cm). Numerous transparent antennas have been developed from such a material at various frequencies, from 800 MHz up to 24 GHz [12]–[16].

The aim of the present work is to extend the investigation up to millimeter wave frequency bands. Hence, the micrometric dimensions of the mesh pattern will be of the same order of magnitude as the working wavelength. In the present study, we focus in particular on the effect of the mesh processing of the ground plane on the microwave performance of an optically transparent  $4 \times 2$  microstrip patch antenna arrays operating at 60 GHz. Accordingly two different transparent antenna arrays are considered here and their microwave performance has been measured and compared with that of an opaque counterpart made of continuous metal films to serve as a reference.

This paper is organized as follows. The design of the antenna arrays is described in Section II. In the subsequent section, the simulation results are presented. Fabrication process of the transparent arrays and opaque counterpart, and the related measurement results are detailed and discussed in Section IV. Finally, conclusions are drawn in Section V.

## II. ANTENNA DESIGN

The antenna studied here is a  $4 \times 2$  rectangular patch antenna array fed by a parallel network in microstrip technology. The substrate used is a  $25.4 \text{ mm} \times 25.4 \text{ mm} \times 0.2 \text{ mm}$  fused quartz with a dielectric permittivity  $\epsilon_r = 3.75$ , a loss tangent  $\tan \delta = 4 \times 10^{-4}$ , and an optical transparency  $T_{sub} = 94\%$  over the entire visible light spectrum. The antenna array dimensions are specified in Fig. 1. The conducting film used is a  $0.8 \mu\text{m}$ -thick silver layer (the best electrical conductor of the periodic table:  $\sigma_{Ag} = 6.1 \times 10^7 \text{ S/m}$  at room temperature [17]) deposited on each side of the fused quartz and three times thicker than the skin depth value  $\delta$  at 60 GHz ( $\delta = 0.26 \mu\text{m}$ ) defined as follows:

$$\delta = \sqrt{\frac{1}{\mu_0 \pi f \sigma_{Ag}}} \quad (1)$$

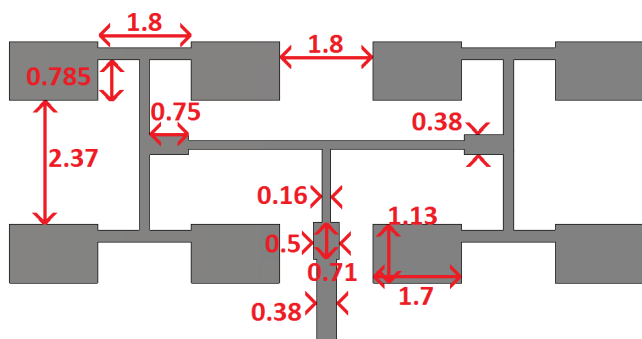


FIGURE 1: Layout and dimensions (in mm) of the antenna array

TABLE 1: Mesh parameters dimensions and related physical characteristics

	Radiating layer	Ground plane
Pitch $p$ ( $\mu\text{m}$ )	100	273
Metal strip width $s$ ( $\mu\text{m}$ )	15	11
Sheet resistance $R'_s$ ( $\Omega/\text{sq}$ )	0.13	0.50
Optical transparency $T(\%)$	67.9	86.6

where  $\mu_0$  is the permeability of the free space, and  $f$  is the operating frequency.

First, two antenna arrays are studied: a transparent mesh antenna array (Array 1) designed with different pitches  $p$  and metal strip widths  $s$  for the radiating layer (to restrict the ohmic loss) and for the ground plane (to improve the optical transparency  $T$ ), respectively (Table 1); and an opaque antenna array made of double-sided continuous silver films (radiating layer and ground plane with  $R_s = 0.02 \Omega/\text{sq}$  and  $T = 0\%$ ) to serve as a reference. The theoretical optical transparency  $T$  and sheet resistance  $R_s$  of the mesh films are computed from equations (2) and (3) derived in [10]:

$$T(\%) = \left(\frac{p-s}{p}\right)^2 \times T_{sub} \quad (2)$$

$$R'_s = \frac{p}{s} \times R_s = \frac{p}{s} \times \frac{1}{\sigma_{Ag} \times t} \quad (3)$$

where  $R_s$  is the sheet resistance of the continuous silver film before its mesh processing and  $t$  is the thickness of the conducting film ( $t = 0.8 \mu\text{m}$ ).

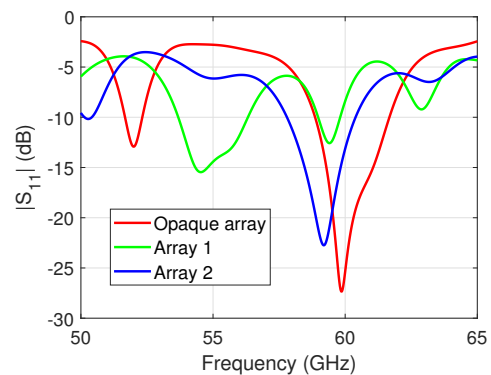


FIGURE 2: Simulated reflection coefficient magnitudes of the three antenna arrays

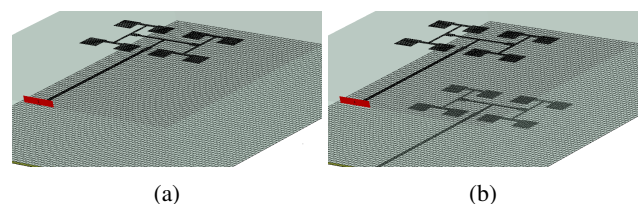


FIGURE 3: 3D-view of (a) the antenna Array 1, and (b) the antenna Array 2 showing the radiating layer footprint into the mesh ground plane

### III. SIMULATION RESULTS

Numerical simulations of the reference (opaque) and mesh (transparent) antenna arrays were performed on the commercial CST Microwave Studio<sup>®</sup> software. The computed reflection coefficients are shown in Fig. 2. As expected and noted in previous studies [15], [16], a frequency shift is noticed between the operating frequency of the opaque antenna array (59.9 GHz) and that of the mesh antenna Array 1 (54.5 GHz). We assign this result to a mesh processing effect of the ground plane. To restrict such frequency shift, the footprint of the radiating layer (consisting of a feeding line, a network and  $4 \times 2$  patches) was printed into the mesh ground plane, precisely facing each other (Fig. 3b). This new mesh antenna array, namely Array 2, has the same structure as Array 1, only the ground plane is modified by adding the radiating layer footprint into this. The computed reflection coefficient of this new antenna array is also presented in Fig. 2. Accordingly, the offset of the operating frequency is narrowed and now close to that of the reference antenna array (59.2 GHz against 59.9 GHz).

The simulated radiation patterns are depicted in Fig. 4. They are plotted at the operating frequency exhibiting the best impedance matching: 59.9 GHz for the opaque antenna array, 54.5 GHz for the antenna Array 1 and 59.2 GHz for the antenna Array 2. If the shape of the radiation patterns does not change strongly after the mesh processing, gains of

the antenna arrays are clearly different with 15.0 dBi for the opaque antenna array, 11.9 dBi for the antenna Array 1 and 13.1 dBi for the antenna Array 2. The simulated radiation efficiency is 89% for the opaque antenna array (at 60 GHz) and 60% for both antenna Arrays 1 (at 55 GHz) and 2 (at 59 GHz). The high efficiency of the opaque antenna array is due to the low dielectric loss of the fused quartz substrate and the low ohmic loss  $R_{loss}$  of the continuous conducting film, as follows:

$$R_{loss} = \sqrt{\frac{\mu_0 \pi f}{\sigma_{eff}}} \quad (4)$$

where  $\sigma_{eff}$  is the effective electrical conductivity of the conducting film ( $\sigma_{eff} = \sigma_{Ag}$  for the continuous silver film and  $\sigma_{eff} = 1/(R'_s \times t)$  for the mesh silver film). Furthermore, we can notice equality in efficiency for both transparent antenna arrays while gains are different. We assign these results to a twin-effect: the operating frequencies are not the same for the antenna arrays (54.5 GHz for Array 1 and 59.2 GHz for Array 2), so their directivities are different (14.1 dBi for Array 1 and 15.2 dBi for Array 2) due to their different electrical sizes. Moreover, the front to back ratio is higher for the antenna Array 2 (12 dB) compared with that of antenna Array 1 (8 dB) due to lower  $R_{loss}$  of the ground plane fitted with the radiating layer footprint. Hence, the printing of the radiating layer footprint into the mesh ground plane improves the radiating layer/ground plane coupling through the fused quartz substrate.

### IV. FABRICATION AND MEASUREMENT RESULTS

The fabrication of such antenna arrays is based on the technological process fully described in [10]. An ultrathin titanium underlayer (5 nm-thick) and a continuous silver film (0.8  $\mu\text{m}$ -thick) are first deposited by the RF sputtering technique on each side of the fused quartz substrate. Subsequently standard photolithographic wet etching processes with the appropriate photomasks are used to pattern the radiating layer and the ground plane. A mask aligner has been used for the photolithography step to provide a strong alignment between the radiating layer photomask and the pattern of the mesh ground plane fitted with the radiating layer footprint (antenna Array 2). And according to Ref. [18], each edge of the radiating layer photomask has to be bordered by a metal strip. Afterwards, stripping of the photoresist leaves the antenna Arrays 1 and 2 with a periodic array of apertures in the respective metal films. Photos of the three fabricated antenna arrays are shown in Fig. 5.

A zoomed view under optical microscopy of one patch of the antenna Array 2 is presented in Fig. 6. A slight misalignment between the mesh of the radiating layer and that of the ground plane of about 30  $\mu\text{m}$  in one direction and 60  $\mu\text{m}$  in the perpendicular direction is observed. Numerical simulations of the antenna Array 2 with two alignment differentials (30  $\mu\text{m}$  and 100  $\mu\text{m}$ , respectively) have been performed (Fig. 7). For small misalignments (differential lower than 100  $\mu\text{m}$ ), the radiation patterns do not evolve,

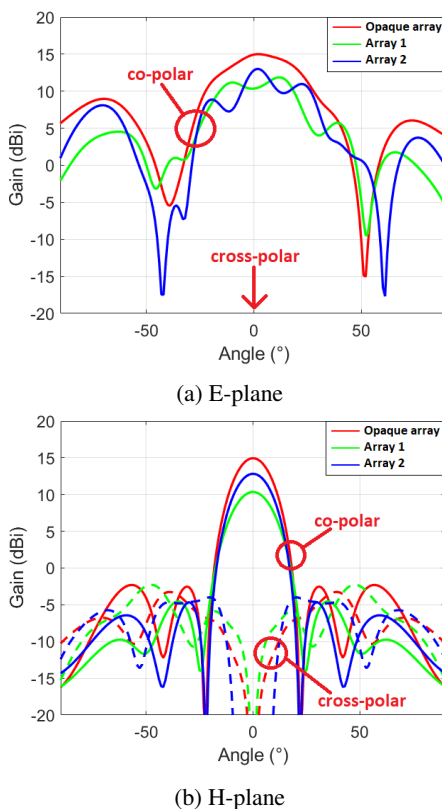


FIGURE 4: Simulated radiation patterns of the three antenna arrays

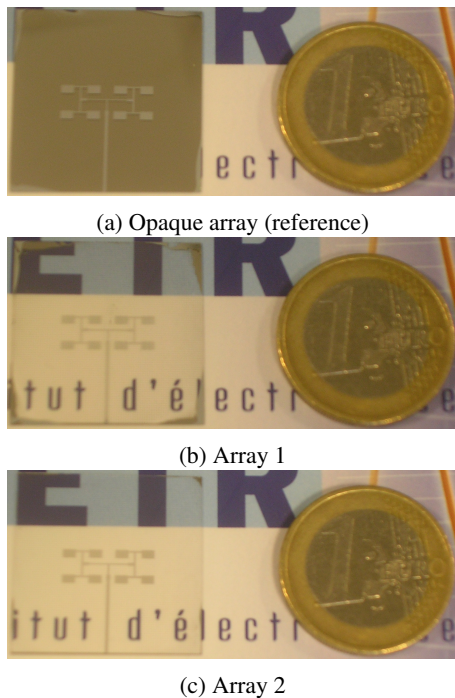


FIGURE 5: Photos of the three antenna arrays placed above the Institute Logo

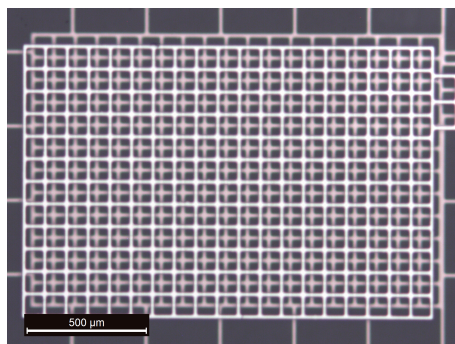


FIGURE 6: Zoomed view under optical microscopy (x100) of a patch of the antenna Array 2

neither in E-plane nor in H-plane. Regarding the reflection coefficient, a slight frequency shift (lower than 300 MHz) is noticed. Therefore a small misalignment has no significant impact on the microwave characteristics of a double-sided micrometric mesh antenna array. In the other hand, its optical transmittance will be impacted locally by such misalignment. It will evolve from  $T = 67.9\%$  (perfect alignment) to  $62.5\%$  (full misalignment).

The ground plane optical transparency of the mesh antenna arrays was measured with a UV/Visible spectrophotometer (Fig. 8).  $T = 83\%$  for the antenna Array 1 and  $T = 86\%$  for the antenna Array 2 (in perfect agreement with the theoretical value, see Table 1) have been recorded over the entire visible light spectrum (400-800 nm). The lowest optical transparency of the antenna Array 1 is due to a larger

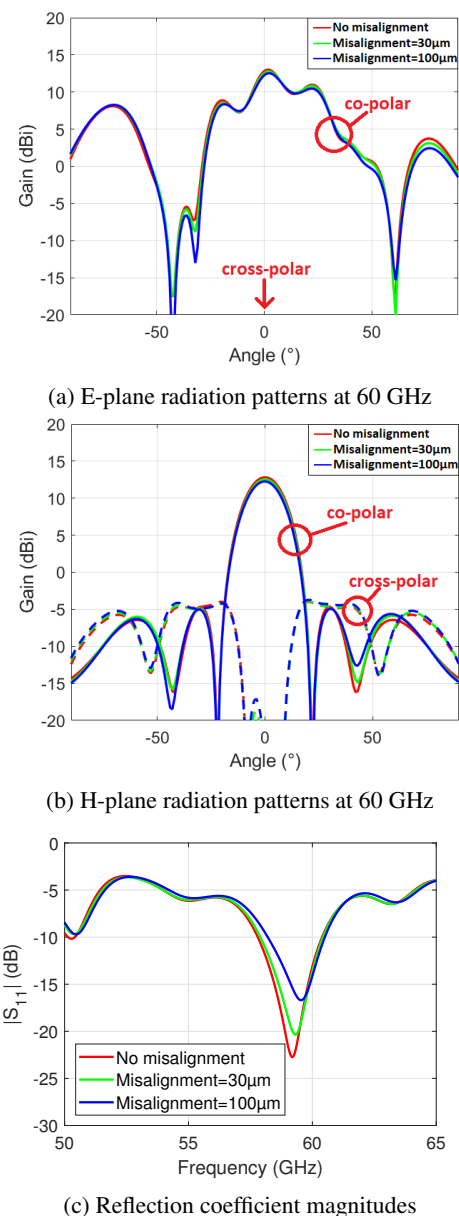


FIGURE 7: Influence of the alignment differential on the antenna Array 2 - Numerical results

silver strip width than the intended value ( $s = 16 \mu\text{m}$  against  $11 \mu\text{m}$ ), mainly as a result of an underetching behavior during the wet etching step.  $16 \mu\text{m}$ -width silver strips give a theoretical optical transparency equal to  $83.3\%$ , which agrees closely with the measured value. It is worth noting that the optical transparency of the mesh radiating layer could not be measured due to the larger UV/Visible beam dimensions ( $7 \text{ mm} \times 1 \text{ mm}$ ) compared with those of an unitary patch ( $1.7 \text{ mm} \times 1.13 \text{ mm}$ , see Fig. 1).

The measured reflection coefficients and radiation patterns of the three fabricated antenna arrays are presented in Figs. 9 and 10, respectively. The measurement results agree well with the numerical ones. Only a small differ-

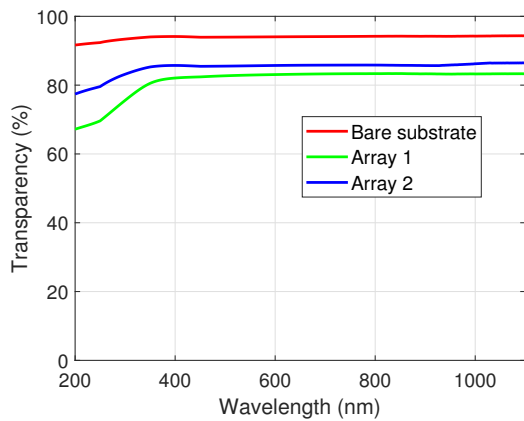


FIGURE 8: Optical transparency measurement of the mesh ground plane of antenna Arrays 1 and 2. Spectrum of the bare fused quartz is also plotted for comparison

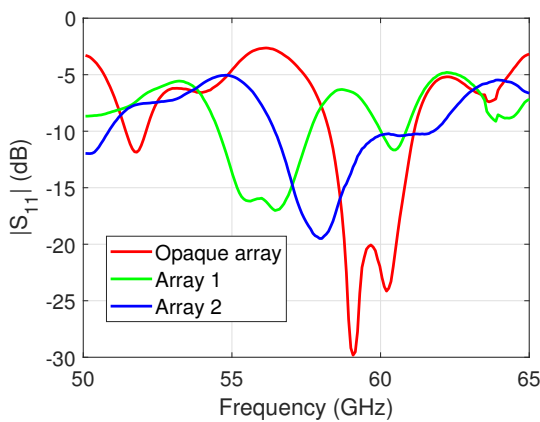
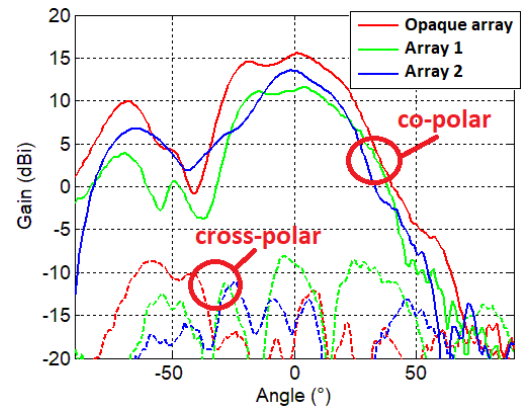


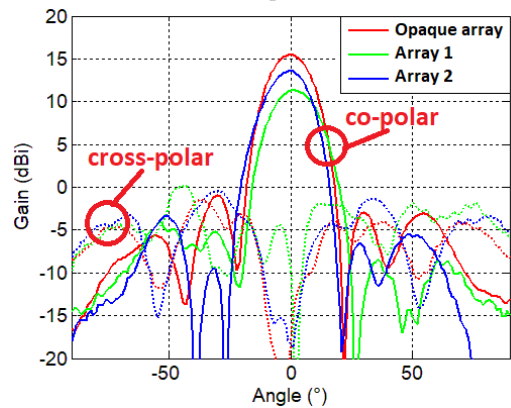
FIGURE 9: Measured reflection coefficient magnitudes of the three antenna arrays

ence is noticed between simulations and measurements in the E-plane due to diffraction effects induced by the V-connector. As disclosed in Section III from simulation results, a strong shift of the resonance frequency for the antenna Array 1 (56.1 GHz) and a lower one for the antenna Array 2 (58.0 GHz) are noticed compared with that of the opaque antenna array (59.7 GHz). Regarding the gain values (Figs. 10 and 11), the opaque antenna exhibits a maximum gain equal to 15.6 dBi (against 15.0 dBi from simulation), 11.6 dBi (against 11.9 dBi from simulation) for the antenna Array 1 and 13.6 dBi (against 13.1 dBi from simulation) for the antenna Array 2. Therefore, the printing of the mesh radiating layer footprint into the mesh ground plane restricts the frequency shift ( $\Delta f = 1.7$  GHz) and improves the gain (difference of 2.0 dB) compared with that an opaque antenna array. The higher gains from measurement compared with those from numerical simulation (between 0.3 dB and 0.6 dB higher) are assigned to the V-connector influence.

The measured H-plane radiation patterns versus frequency



(a) E-plane



(b) H-plane

FIGURE 10: Measured radiation patterns of the three antenna arrays at resonance frequency

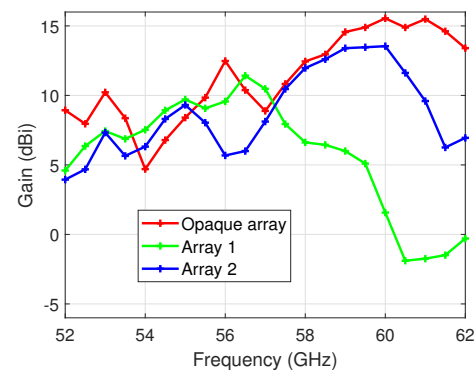


FIGURE 11: Maximum gains versus frequency of the three antenna arrays

are displayed in Fig. 12. Once more, the large frequency shift exhibited by the mesh antenna Array 1 and the lower one by the mesh antenna Array 2 are clearly highlighted. Moreover, the use of the footprint also reduces the side lobe levels compared with those exhibited by the antenna Array 1. Accordingly, the radiation pattern of the antenna Array 2 is very close to that of the opaque antenna array. Additionally,

a mesh antenna array fabricated without footprint into the mesh ground plane exhibits a gain value drastically reduced at 60 GHz (close to 0 dBi, see Fig. 11). Whereas the use of the mesh radiating layer footprint into the mesh ground plane maintains a high level of gain at 60 GHz (13.6 dBi against 15.6 dBi for the opaque antenna array). Nevertheless, our technology also puts limits at higher operating frequencies (100 GHz and above). In that case, the reduction of the mesh pitch will be needed at the expense of the optical transparency.

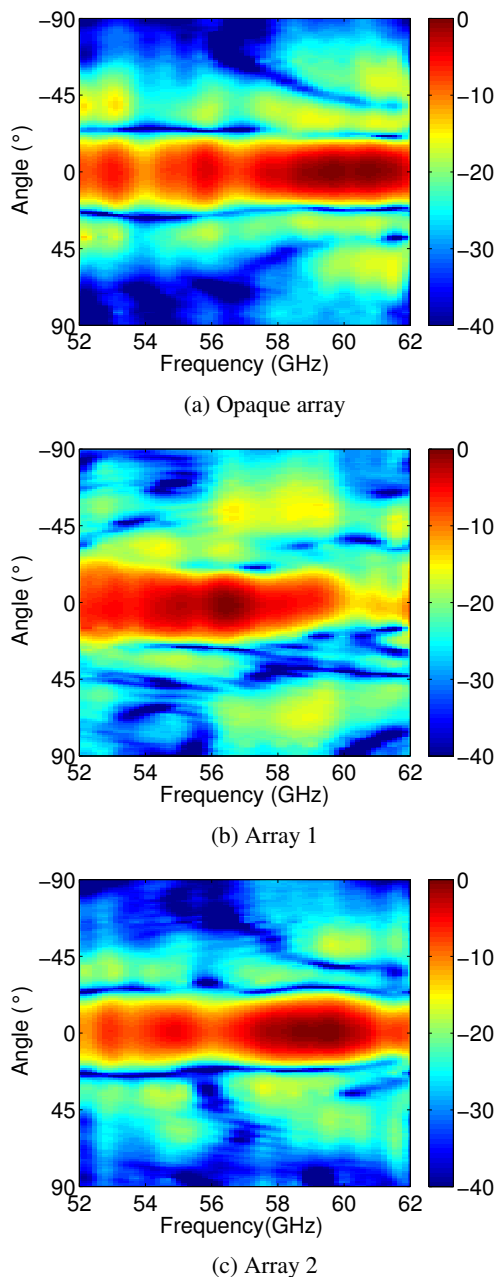


FIGURE 12: Measured H-plane radiation patterns versus frequency (normalized gain (dBi))

Our results can be compared with those of a  $4 \times 1$  optically transparent patch antenna array based on a similar technology (micrometric mesh metal film printed on a fused quartz substrate) without any footprint into the mesh ground plane [19] (Table 2). Hence a 3.2 GHz resonant frequency shift is measured between the transparent antenna array and the reference and opaque counterpart. The side lobe level remains high (-7 dB) due to the mesh processing. On the one hand, the gain difference between the transparent antenna array and the reference counterpart is equal to 0.5 dB because of narrower mesh patterns used (pitch from  $100 \mu\text{m}$  to  $200 \mu\text{m}$ , against  $100 \mu\text{m}$  to  $300 \mu\text{m}$  in the present work) which restrict the ohmic loss. On the other hand, the optical transparency of such antenna array is also reduced (37% and 75% against 68% and 87% in the present work) as explained above. A comparison with additional current 60 GHz antenna arrays is also given in Table 2.

TABLE 2: Dimensions and performance of different 60 GHz antenna arrays

Technology (elem. number)	Dimensions (mm $\times$ mm)	Gain (dBi)	Efficiency (%)	Optically transparent
LTCC [20] ( $8 \times 8$ )	$47 \times 31$	22	55	No
Teflon [21] ( $2 \times 2$ )	$10 \times 10$	11	91	No
Roger 5880/6010 [22] ( $4 \times 4$ )	$20 \times 25$	16.5	87	No
Fused quartz [19] ( $4 \times 1$ )	$7 \times 11$	9.5	/	Yes (37% / 75%)
Present work ( $4 \times 2$ )	$25 \times 25$	13.6	60	Yes (68% / 87%)

## V. CONCLUSION

Optically transparent  $4 \times 2$  microstrip patch antenna arrays operating at 60 GHz and made from double-sided micrometric mesh silver films have been designed, fabricated and measured. Their performance was compared with that of an opaque antenna array made of double-sided continuous silver films serving as reference (measured resonance frequency  $f = 59.7$  GHz and measured gain equal to 15.6 dBi). As expected, the transparent antenna array made from a conventional mesh processing of the radiating layer and ground plane exhibits a large resonance frequency shift ( $\Delta f = 3.6$  GHz) and a lower gain (11.6 dBi). By adding the radiating layer footprint into the mesh ground plane and precisely facing each other, a lower resonance frequency shift is achieved ( $\Delta f = 1.7$  GHz) coupled with a higher gain value (13.6 dBi). Moreover, the radiating layer and its footprint into the ground plane do not need to be perfectly aligned (a misalignment up to  $100 \mu\text{m}$  is allowed at 60 GHz) to provide strong performance at microwaves, even if it impacts slightly and locally the optical transparency of the sample (transmittance loss of about 5%).

## REFERENCES

- [1] K. Fujimoto, "Small antennas," in Encyclopedia of RF and Microwave Engineering, John Wiley & Sons, 2005.

- [2] J. L. Volakis, C. C. Chen, K. Fujimoto, "Small antennas: miniaturization techniques & applications," in New York: McGraw-Hill., vol. 1, 2010.
- [3] M. Justen, C. Bonzon, K. Ohtani, M. Beck, U. Graf, J. Faist, "2D patch antenna array on a double metal quantum cascade laser with >90% coupling to a Gaussian beam and selectable facet transparency at 1.9 THz," in *Optics Letters*, vol. 41, no. 19, pp. 4590–4592, 2016.
- [4] T. Yasin, R. Baktur, C. Furse, "A study on the efficiency of transparent patch antennas designed from conductive oxide films," in 2011 IEEE International Symposium on Antennas and Propagation (APSURSI), pp. 3085–3087, 2011.
- [5] M. Awalludin, M. T. Ali, M. H. Mamat, "Transparent antenna using aluminum doped zinc oxide for wireless application," in 2015 IEEE Symposium on Computer Applications Industrial Electronics (ISCAIE), pp. 33–36, 2015.
- [6] F. Colombel, X. Castel, M. Himdi, G. Legeay, S. Vigneron, E. Motta Cruz, "Ultrathin metal layer, ITO film and ITO/Cu/ITO multilayer towards transparent antenna," in *IET Science, Measurement & Technology*, vol. 3, pp. 229–234, 2009
- [7] A. Klöppel, B. Meyer, J. Trube, "Influence of substrate temperature and sputtering atmosphere on electrical and optical properties of double silver layer systems," in *Thin Solid Films*, vol. 392, no. 2, pp. 311–314, 2001.
- [8] H. J. Song, T. Y. Hsu, D. F. Sievenpiper, H. P. Hsu, J. Schaffner, E. Yasan, "A Method for Improving the Efficiency of Transparent Film Antennas," in *IEEE Antennas and Wireless Propagation Letters*, vol. 7, pp. 753–756, 2008.
- [9] M. S. A. Rani, S. K. A. Rahim, M. R. Kamarudin, T. Peter, S. W. Cheung, B. M. Saad, "Electromagnetic Behaviors of Thin Film CPW-Fed CSRR Loaded on UWB Transparent Antenna," in *IEEE Antennas and Wireless Propagation Letters*, vol. 13, pp. 1239–1242, 2014.
- [10] J. Hautcoeur, X. Castel, F. Colombel, R. Benzerga, M. Himdi, G. Legeay, E. Motta-Cruz, "Transparency and electrical properties of meshed metal films," in *Thin Solid Films*, vol. 519, no. 11, pp. 3851–3858, 2011.
- [11] T. Yasin, R. Baktur, C. Furse, "A comparative study on two types of transparent patch antennas," in 2011 General Assembly and Scientific Symposium, (URSI), pp. 1–4, 2011.
- [12] J. Hautcoeur, F. Colombel, X. Castel, M. Himdi, E. Motta Cruz, "Optically transparent monopole antenna with high radiation efficiency manufactured with a silver grid layer (AgGL)," in *Electronics Letters*, vol. 45, pp. 1014–1016, 2009.
- [13] J. Hautcoeur, X. Castel, F. Colombel, M. Himdi, E. Motta-Cruz, "Comparison of the microwave performance of transparent wire monopole antennas based on silver films," in *Journal of Electronic Materials*, vol. 42, no. 3, pp. 552–557, 2013.
- [14] J. Hautcoeur, F. Colombel, M. Himdi, X. Castel, E. Motta Cruz, "Large and optically transparent multilayer for broadband H-shaped slot antenna," in *IEEE Antennas and Wireless Propagation Letters*, vol. 12, no. 1, pp. 933–936, 2013.
- [15] A. Martin, X. Castel, O. Lafond, M. Himdi, "Optically transparent frequency-agile antenna for X-band applications," in *Electronics Letters*, vol. 51, pp. 1231–1233, 2015.
- [16] Q. H. Dao, R. Braun, B. Geck, "Design and investigation of meshed patch antennas for applications at 24 GHz," in *Proceedings of the 45th European Microwave Conference (EuMW)*, Paris, France, pp. 1499–1502, 2015.
- [17] W. Haynes, "CRC Handbook of Chemistry and Physics," in CRC Press, Boca Raton, FL, 2016–2017.
- [18] J. Hautcoeur, F. Colombel, X. Castel, M. Himdi, E. Motta-Cruz, "Radiofrequency performances of transparent ultra-wideband antennas," in *Progress In Electromagnetics Research C*, vol. 22, pp. 259–271, 2011.
- [19] J. Hautcoeur, L. Talbi, K. Hettak, M. Nedil, "60 GHz optically transparent microstrip antenna made of meshed AuGL material," in *IET Microwaves, Antennas Propagation*, vol. 8, no. 13, pp. 1091–1096, 2014.
- [20] J. Xu, Z. N. Chen, X. Qing, W. Hong, "Bandwidth enhancement for a 60 GHz substrate integrated waveguide fed cavity array antenna on LTCC," in *IEEE Transactions on Antennas and Propagation*, vol. 59, no. 3, pp. 826–832, 2011.
- [21] T. Seki, N. Honma, K. Nishikawa, K. Tsunekawa, "Millimeter-wave high-efficiency multilayer parasitic microstrip antenna array on teflon substrate," in *IEEE Transactions on Microwave Theory and Techniques*, vol. 53, no. 6, pp. 2101–2106, 2005.
- [22] Y. Li, K. M. Luk, "Dense dielectric patch antenna array," in *IEEE Transactions on Antennas and Propagation*, vol. 62, no. 2, pp. 960–963, 2014.



papers, 2 patents and 10 conference presentations.

ALEXIS MARTIN received his M.S. degree in Electronics and Telecommunication from University of Rennes 1, Rennes, France in 2014 and his Ph.D. degree in Electronics and Telecommunication from University of Rennes 1, France in 2017. He is a postdoctoral fellow at University of Ontario Institute of Technology, Oshawa, Canada from 2018. He is working on optically transparent and active antennas, and active radiofrequency circuits. He is author and co-author of 5 international



in conference proceedings. He has also authored/coauthored three book chapters. He holds 7 patents in the area of antennas.

OLIVIER LAFOND received his M. S. degree in radar and telecommunications from the University of Rennes, Rennes, France, in 1996, and the Ph.D. degree in Signal Processing and Telecommunications from the University of Rennes 1, Rennes, France, in 2000. Since October 2002, he has been an Associate Professor with the Institute of Electronics and Telecommunications of Rennes (IETR), University of Rennes 1. He has authored or coauthored of 40 journal papers and 63 papers

His research activities deal with passive and active millimeter-wave multilayer antennas and circuits, reconfigurable antennas, inhomogeneous lenses for shaping radiation patterns with active devices, imaging antenna systems.



and active millimeter-wave antennas. His research also include development of new architectures of antenna arrays, and new three-dimensional (3-D) antenna technologies. He was Laureat of the 2d National Competition for the Creation of Enterprises in Innovative Technologies in 2000 (Ministry of Industry and Education). In March 2015 he received the JEC-AWARD at Paris on Pure composite material antenna embedded into a motorhome roof for the Digital Terrestrial Television reception.

MOHAMED HIMDI received the Ph.D. degree in signal processing and telecommunications from the University of Rennes 1, France in 1990. Since 2003, he has been a Professor with the University of Rennes 1, and the Head of the High Frequency and Antenna Department until 2013, of IETR. He has authored or coauthored 112 journal papers and over 255 papers in conference proceedings. He has also coauthored 9 book chapters. He holds 39 patents. His research activities concern passive



XAVIER CASTEL received the Ph.D. degree in Material Science from the University of Rennes 1, Rennes, in 1997. He was an Associate Professor with the Technological Institute of Saint-Brieuc, University of Rennes 1, Saint-Brieuc, France from 1999 to 2016, and a Researcher with the Institute of Electronics and Telecommunications of Rennes, University of Rennes 1. He was nominated as Full Professor in 2017 at the same Institutes. He is currently Cohead of the 'Functional

Materials' Team in the 'Antennas & Microwave Devices' Department. He is the author and coauthor of ~50 international papers, more than 200 conference presentations, and holds 13 patents. He was a recipient and co-recipient of 7 scientific Awards.

His main research interests include the elaboration of advanced materials (transparent materials and transparent conducting oxides; superconductors; semiconductors, composite materials) for microwave applications, their physical-chemical characterizations (electrical, optical, structural, microstructural, morphological properties, etc.) and the fabrication of the related microwave devices (by photolithographic technique, wet-etching process, lift-off process and laser micro-etching).

• • •